

# The role of mobility in bulk heterojunction solar cells

Feng Xu<sup>1</sup> and Dadong Yan<sup>2,a)</sup>

<sup>1</sup>Beijing National Laboratory for Molecular Sciences (BNLMS), Institute of Chemistry, Chinese Academy of Sciences, Beijing 100190, China

<sup>2</sup>Department of Physics, Beijing Normal University, Beijing 100875, China

(Received 7 June 2011; accepted 24 August 2011; published online 14 September 2011)

In this letter, we employ a three-dimensional master equation calculation to investigate the mobility dependence of bulk heterojunction (BHJ) solar cell performance. By taking energetic disorder and morphology into consideration, we show mobility-enhanced device efficiency with a remarkable charge transport loss induced by molecular disorder and an open circuit voltage loss in high mobility region due to morphological defect-assisted bimolecular recombination. The result suggests that the description of interfacial processes is crucial in the modeling of BHJ photovoltaic devices. © 2011 American Institute of Physics. [doi:10.1063/1.3639273]

Organic bulk heterojunction (BHJ) solar cells are promising candidates for photovoltaic application as they can be manufactured with large-area printing techniques at low cost. Recent developments have lead to photovoltaic devices with power conversion efficiencies of 7.73%,<sup>1</sup> a value which is about to meet the commercialization demand of these devices. Nevertheless, fundamental aspect of charge transport has to be better understood to further improve the device performance, since better charge transport allows for thicker films that have higher photocurrents.<sup>2</sup>

A central role for charge transport in organic material is played by mobility, which originates from charge carrier hopping in an energetically disordered landscape.<sup>3</sup> The disordered energy, equivalently representing the molecular disorder in organic material (e.g., disordered molecular packing and orientation), is usually assumed to be Gaussian distributed. For neat material, energetic disorder is known to have a strong influence upon mobility  $\mu \propto \exp(-c\sigma^2/T^2)$  with  $\sigma$  the Gaussian width,<sup>3,4</sup> and the resulting current channeling is filamentary-like around energetic barriers with diameters close to the one of BHJ network.<sup>5</sup> Therefore, for BHJ blends that exhibit remarkable donor-acceptor (D-A) interfaces, photocurrents are more likely to be blocked and trapped by energetic disorder, which will lead to a more pronounced mobility-dependent device performance. Unfortunately, previous studies have failed to consider this effect, as they are limited by zero-disorder assumption.<sup>6-8</sup> Hence, the role of mobility in BHJ solar cells needs to be reexamined with an energetically disordered model.

In this letter, we employ a three-dimensional (3D) master equation approach to calculate the mobility dependence upon device performance. The simulation space is a lattice system of dimensions 50 nm × 50 nm × 50 nm with lattice constant  $a = 1$  nm, maximum hopping distance being  $\sqrt{3}a$  and period boundary conditions applied in  $x$  and  $y$  directions. The electrodes are at  $z = 1$  nm and  $z = 50$  nm planes. The BHJ morphology is generated by cellular automata approach,<sup>9</sup> and each site energy contains a random energy from Gaussian distribution.

In the calculation, three master equations are needed for the three particles involved, namely, exciton, hole, and electron. For exciton, the stationary master equation for each bulk site  $i$  can be written as

$$\sum_{j \neq i} [w_{ji}S_j - w_{ij}S_i] + G^S - R^S S_i = 0. \quad (1)$$

Here,  $S$  denotes the exciton occupation probability;  $G^S$  is the exciton generation rate due to incident light and  $R^S$  is the decay rate that determines the exciton diffusion length. Exciton hopping follows Förster energy transfer<sup>10</sup> so that  $w_{ij} = w_0(R_0/R_{ij})^6 \text{Bol}(E_j^{\text{ex}} - E_i^{\text{ex}})$  with  $E^{\text{ex}}$ ,  $w_0$ ,  $R_0$ , and  $R_{ij}$  being the site energy, the hopping frequency, the exciton localization radius, and the hopping distance, respectively;  $\text{Bol}(E) = \exp(-E/k_B T)$  for  $E > 0$  and  $\text{Bol}(E) = 1$  otherwise. For the D-A interfacial sites, the left hand side of Eq. (1) should add the contributions  $-k_{\text{ed}}^i S_i(1 - p_i)$  and  $R_{\text{br}}^i$  of exciton dissociation (ED) and bimolecular recombination (BR), respectively. In previous studies, the ED rate  $k_{\text{ed}}$  is assumed to follow Onsager theory,<sup>11</sup> where dissociation is treated as temperature and field assisted diffusive escape of geminate pairs (GP). Contrary to this theory, however, transient experiments have showed that the field dependence of this escape in conjugated polymer is vanishingly small and the initial exciton dissociation into GP contributes most to the field dependence.<sup>12</sup> Therefore,  $k_{\text{ed}}$  in donor should be given by the thermal-assisted energy transfer from exciton to GP with an average separation distance of  $\hat{l}_0 a$  (along field direction once  $u_i \neq u_j$ ; otherwise the initial separation is assumed in the  $x$ - $y$  plane),

$$k_{\text{ed}}^i = k_0 \sum_k \exp \left[ \frac{-E_B + (u_k - u_i)\hat{l}_0 + \Delta}{k_B T} \right] / \sum_k 1. \quad (2)$$

Here,  $E_B$  is the binding energy loss during the initial separation,  $u$  is the electric potential self-consistently solved by 1D Poisson equation,  $\Delta$  is the lowest unoccupied molecular orbital difference between donor and acceptor, and  $k$  is any neighboring acceptor site of donor site  $i$ .

For charge carriers (e.g., hole), the stationary Pauli master equation for each bulk site  $i$  is of a similar form

<sup>a)</sup> Author to whom correspondence should be addressed. Electronic mail: yandd@bnu.edu.cn.

$$\sum_{j \neq i} [v_{ji} p_j (1 - p_i) - v_{ij} p_i (1 - p_j)] = 0. \quad (3)$$

Here,  $p$  is the hole occupation probability; charge hopping is assumed as thermally assisted tunneling<sup>13</sup> thus  $v_{ij} = v_0 \exp(-2\alpha R_{ij}) \text{Bol}(E_j^c + u_j - E_i^c - u_i)$  with  $v_0$ ,  $\alpha$ , and  $E^c$  being the hopping frequency, the inverse localization length of localized wave functions, and the carrier site energy, respectively. For the D-A interfacial sites, the left hand side of Eq. (3) should add the contributions  $k_{\text{ed}}^i S_i (1 - p_i)$  and  $-R_{\text{br}}^i$  of ED and BR, respectively. The BR rate can be written as thermally assisted attraction of GP from a distance of  $\hat{l}_0 a$  to zero

$$R_{\text{br}}^i = R_0 p_i \sum_k n_k \exp\left[\frac{E_B - (u_k - u_i) \hat{l}_0}{k_B T}\right] / \sum_k 1. \quad (4)$$

Additionally, the sites next to electrodes are assumed to be in equilibrium with the metal. We have

$$p_i = N_D a^3 / \{1 + \exp[(E_i^c - E_F)/k_B T]\}, \quad (5)$$

where  $N_D$  is the effective density of states of donor and  $E_F$  is the Fermi level of the contact metal.

The above master equations can be iteratively solved analogous to Yu *et al.*<sup>14</sup> By solving Eq. (1), the ED yield is obtained and converted to the charge generation yield in Eq. (3). The simultaneous equations of holes [Eq. (3)] and electrons [similar to Eq. (3), not shown] are solved and the current density can be obtained as

$$J_{\text{hop}} = \sum_i \sum_{j \neq i} q v_{ij} a^3 P_i (1 - P_j) R_{ijz} / V \quad (P = p, n), \quad (6)$$

with  $q$  and  $V$  being the charge of carriers and the total volume, respectively. Averages over a number of different disorder configurations are taken until the standard deviations of current densities are within 0.2 A/m<sup>2</sup>. Mobilities are calculated as in Ref. 4 under short circuit conditions in order to compare directly with the ones in neat material. In low mobility region ( $\mu \leq \mu_c$ , with  $\mu_c = 8.5 \times 10^{-7}$  m<sup>2</sup>/Vs), mobility is increased by reducing energetic disorder from 154 meV to zero; in high mobility region with no disorder ( $\mu > \mu_c$ ), mobility is enhanced by raising charge hopping frequency from 1 to  $10^4$  times.

The main results of the calculation are summarized in Fig. 1, where the device performance indicators are plotted as a function of mobility. From the results, it is apparent that for  $\mu \leq \mu_c$ , mobility acts a positive role upon  $I$ - $V$  characteristics. For  $\mu > \mu_c$ , device efficiency (proportional to  $P_{\text{max}}$ ) and short circuit current ( $J_{\text{sc}}$ ) both feature a plateau with increasing mobility whereas the open circuit voltage ( $V_{\text{oc}}$ ) shows a reduction. It is observed that the fill factor and  $V_{\text{oc}}$  are relatively insensitive to mobility and the  $J_{\text{sc}}$  contributes most to the mobility dependence of device efficiency.

The physical origin of the observations becomes clear by looking at Fig. 2. At applied voltage of  $U = 0$ , the charge generation yield increases slightly with decreasing disorder and saturates at high mobilities, indicating an detrimental effect of disorder to ED. On the contrary, the BR rate shows a sharp decrease, which is a sign of attenuating space charge

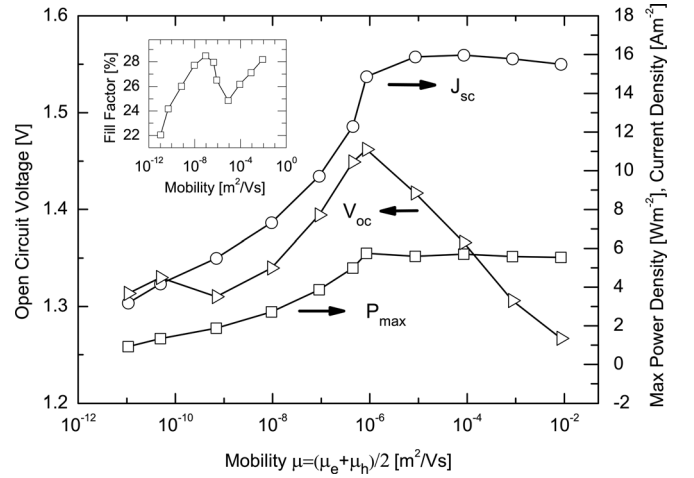


FIG. 1. Calculated mobility dependence of the maximum power output ( $P_{\text{max}}$ ), short circuit current ( $J_{\text{sc}}$ ), open circuit voltage ( $V_{\text{oc}}$ ), and fill factor (inset). The symbols are calculated with a convergence criterion  $10^{-8}$ , an *ab initio* separation distance  $\hat{l}_0 a = 2$  nm, a donor excitation generation rate  $G_D^S = 3.6 \times 10^{28} \text{ m}^{-3} \text{ s}^{-1}$ , and a ratio  $\mu_h/\mu_e = 8$ . The lines are a guide to the eye.

accumulation. This observation can be attributed to disorder effect, by virtue of its role of blocking transport pathways and trapping photocurrents inside the BHJ. The trapped charges, unable to be collected by the electrodes to contribute to  $J_{\text{sc}}$ , accumulate in the BHJ and annihilate through BR. Therefore, the five times increase in  $J_{\text{sc}}$  can be identified as the photocurrents released from the pathways that are initially blocked by formidable energetic barriers.

In Fig. 2, the charge generation and BR rate at  $U = 1.4$  V are also displayed. For  $V_{\text{oc}} < 1.4$  V (cf. Fig. 1), BR exceeds charge generation, indicating significant recombination of both the photocurrent and dark-injected current. At the optimum mobility for  $V_{\text{oc}}$ , BR has a minimum rate that is less than charge generation. Therefore, it can be concluded that  $V_{\text{oc}}$  is primarily influenced by BR. The variance in BR actually originates from electron concentration. As depicted in the inset of Fig. 2, electron concentration shows a rapid decrease for  $\mu \leq \mu_c$  and a sharp increase for  $\mu > \mu_c$ . The former can be explained by disorder-induced space charge

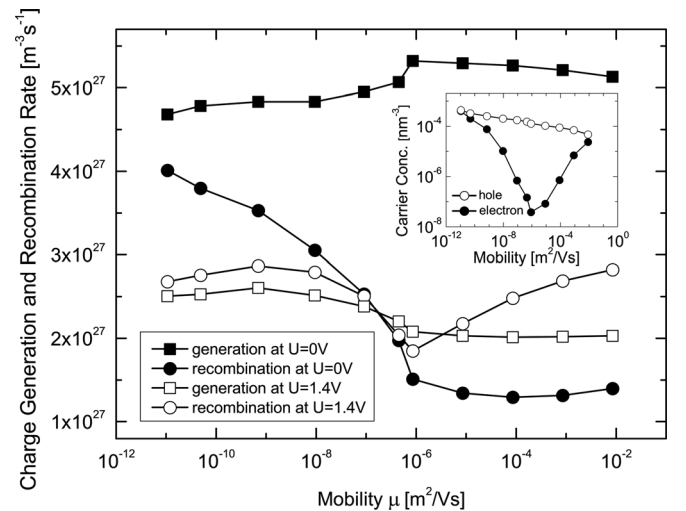


FIG. 2. Charge generation and recombination rates as a function of mobility under various applied voltage  $U$ . The inset shows the mobility dependence of carrier concentrations at  $U = 1.4$  V. The lines are a guide to the eye.

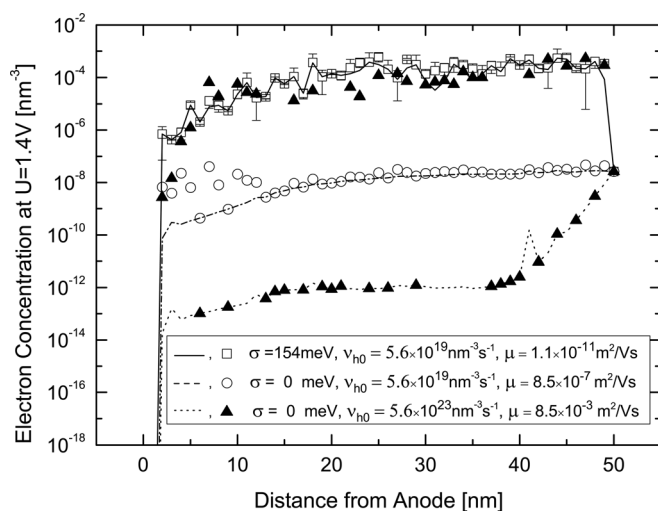


FIG. 3. Electron distribution at  $U = 1.4$  V for the three characteristic mobilities in Fig. 1 (symbols). The lines are the ones that morphology defects are excluded from averaging.

accumulation, but the latter is quite unusual. By depicting the electron distribution at  $U = 1.4$  V (symbols in Fig. 3) and examining the layers with abnormally high carrier concentrations at  $\mu = 8.5 \times 10^{-3} \text{ m}^2/\text{Vs}$ , we find that the increase in electron concentration comes from the morphology defects that are isolated from electrodes. If these defects are excluded from averaging, the concentration would show a monotonically decrease with mobility (lines in Fig. 3), indicating a monotonically increasing  $V_{oc}$  with mobility for a defect-free morphology. Bearing in mind that charge extraction is limited on these defects, it is not surprising that their concentrations are eventually close to the ones with significant disorder. Here, we conclude that both energetic disorder and BHJ defects are detrimental to  $V_{oc}$  due to BR.

Remarkably, our calculation results confirm that energetic disorder is detrimental to  $V_{oc}$  (Ref. 15) and support the idea that more ordered materials provide higher efficiencies.<sup>16</sup> Furthermore, the results suggest that disorder and morphology defects are responsible for “the missing  $V_{oc}$ ” (Ref. 17) in BHJ devices. However, these findings are quite different from the drift-diffusion model, where a global mobility is explicitly incorporated into ED and BR to result in a counterintuitive optimum mobility for device efficiency and a decreasing  $V_{oc}$  with mobility.<sup>6,7</sup> This discrepancy may

originate from the mobility-enhanced BR rate and distribution of separation distances assumed in the drift-diffusion model,<sup>8</sup> and it suggests that the description of interfacial processes is crucial in predicting the mobility dependence of device performance.

In summary, we employ a master equation approach to correlate energetic disorder and 3D morphology to the mobility dependence of BHJ solar cell performance. The device efficiency is found to increase with mobility and be dominated by the variance in  $J_{sc}$ . A remarkable photocurrent loss is identified due to disorder in organic material, and a further  $V_{oc}$  loss is attributed to disorder effect and morphological defect-assisted bimolecular recombination. Furthermore, a comparison with previous studies suggests that the description of interfacial processes is important in the modeling of BHJ solar cells.

This work is supported by National Natural Science Foundation of China (NSFC) 20973176, 20990234, 50821062, 20874111, and 973 Program of the Ministry of Science and Technology (MOST) 2011CB808502.

<sup>1</sup>H. Y. Chen, J. Hou, S. Zhang, Y. Liang, G. Yang, Y. Yang, L. Yu, Y. Wu, and G. Li, *Nature Photon.* **3**, 649 (2009).

<sup>2</sup>H. Hoppe and N. S. Sariciftci, *J. Mater. Res.* **19**, 1924 (2004).

<sup>3</sup>H. Bässler, *Phys. Status Solidi B* **175**, 15 (1993).

<sup>4</sup>W. F. Pasveer, J. Cottaar, C. Tanase, R. Coehoorn, P. A. Bobbert, P. W. M. Blom, D. M. de Leeuw, and M. A. J. Michels, *Phys. Rev. Lett.* **94**, 206601 (2005).

<sup>5</sup>E. Tutiš, I. Batistić, and D. Berner, *Phys. Rev. B* **70**, 161202 (2004).

<sup>6</sup>M. M. Mandoc, L. J. A. Koster, and P. W. M. Blom, *Appl. Phys. Lett.* **90**, 133504 (2007).

<sup>7</sup>C. Deibel, A. Wagenpfahl, and V. Dyakonov, *Phys. Status Solidi (RRL)* **2**, 175 (2008).

<sup>8</sup>T. Kirchartz, B. E. Pieters, K. Taretto, and U. Rau, *Phys. Rev. B* **80**, 035334 (2009).

<sup>9</sup>P. Peumans, S. Uchida, and S. R. Forrest, *Nature* **425**, 158 (2003).

<sup>10</sup>B. Movaghar, M. Grünwald, B. Ries, H. Bässler, and D. Würtz, *Phys. Rev. B* **33**, 5545 (1986).

<sup>11</sup>L. Onsager, *Phys. Rev.* **54**, 554 (1938).

<sup>12</sup>M. Weiter, H. Bässler, V. Gulbinas, and U. Scherf, *Chem. Phys. Lett.* **379**, 177 (2003).

<sup>13</sup>A. Miller and E. Abrahams, *Phys. Rev.* **120**, 745 (1960).

<sup>14</sup>Z. G. Yu, D. L. Smith, A. Saxena, R. L. Martin, and A. R. Bishop, *Phys. Rev. B* **63**, 085202 (2001).

<sup>15</sup>G. Garcia-Belmonte and J. Bisquert, *Appl. Phys. Lett.* **96**, 113301 (2010).

<sup>16</sup>R. A. Street, *Appl. Phys. Lett.* **93**, 133308 (2008).

<sup>17</sup>M. C. Scharber, D. Mühlbacher, M. Koppe, P. Denk, C. Waldauf, A. J. Heeger, and C. J. Brabec, *Adv. Mater.* **18**, 789 (2006).